Surface properties and bacterial adhesion on polyurethane central catheters: Impact of ethanol lock solution

A. Khzam, J. Saunier, Morgan Guilbaud, J.M. Herry, A. Dazzi, L. Tortolano, L. Carpentier, A. Mignot, N. Yagoubi

▶ **To cite this version:**

A. Khzam, J. Saunier, Morgan Guilbaud, J.M. Herry, A. Dazzi, et al.. Surface properties and bacterial adhesion on polyurethane central catheters: Impact of ethanol lock solution. Biomaterials Advances, 2023, 146, pp.213281. 10.1016/j.bioadv.2023.213281 . hal-04303122

HAL Id: hal-04303122
https://hal.inrae.fr/hal-04303122v1

Submitted on 2 Sep 2024

HAL is a multi-disciplinary open access archive for the deposit and dissemination of scientific research documents, whether they are published or not. The documents may come from teaching and research institutions in France or abroad, or from public or private research centers.

L'archive ouverte pluridisciplinaire **HAL**, est destinée au dépôt et à la diffusion de documents scientifiques de niveau recherche, publiés ou non, émanant des établissements d'enseignement et de recherche français ou étrangers, des laboratoires publics ou privés.

Surface properties and bacterial adhesion on polyurethane central catheters: Impact of ethanol lock solution

A. Khzam[1], J. Saunier[1], M. Guilbaud[2], J.M. Herry[2], A. Dazzi[3], L. Tortolano[1,4], L. Carpentier[5], A. Mignot[5], N. Yagoubi[1]

[1]Matériaux et Santé, UFR de pharmacie, Université Paris Saclay

[2] Université Paris-Saclay, INRAE, AgroParisTech, UMR SayFood, 91300 Massy, France

[3] Université Paris-Saclay, CNRS, Institut de Chimie Physique, 91405, Orsay, France

[4] Department of Pharmacy, Henri Mondor Hospital, Créteil, France

[5] Vygon, Ecouen, France

Abstract

It was shown in the literature that ethanol locks have a positive effect on preventing catheter-related infections in patients with central venous catheters without causing any microbial resistance. However, ethanol is known to interact with polyurethanes. The consequences of this interaction on the catheter surface properties were studied as it can impact the biocompatibility of the material and the adhesion phenomena onto the surface. No physical and chemical degradation was put into evidence, but low molecular weight compounds such as additives were extracted from the catheter bulk or migrated and exudated onto its surface. Nevertheless, as far as bacterial adhesion is concerned, after the catheter was locked and the lock removed, the surface modifications promoted no adhesion.

Keywords

Central venous catheter – bacterial adhesion – ethanol lock – surface – migration - additive

1. Introduction

Polyurethane (PU) is a large family of polymers widely used in the medical field, especially in the fabrication of implantable medical devices, because of PU's interesting mechanical and chemical properties and biocompatibility. The central venous catheter is one of the most used medical devices made of polyurethane.

Central venous catheters (CVCs) are commonly used in the care of critically ill patients. These devices are flexible tubes inserted into a vein of the central vasculature to administer medications such as chemotherapeutic agents, antibiotics, parenteral nutrition, and blood products. CVCs can also be used for blood sampling. The CVC surface state (chemical composition, charge, hydrophilicity, and topography) is substantial for the device's biocompatibility. In the case of venous catheters, which can be implanted for several months, the catheter surface may impact thrombosis [1,2] and bacterial adhesion [3].

Many low molecular weight compounds may be present in extruded polyurethane catheters, such as additives (antioxidants and lubricants), oligomers, and residual monomers, which can migrate to the surface under certain conditions and significantly influence the surface properties [4,5]. These catheters may also contain an inorganic filler that acts as a radio-opaque agent (for example, barium sulfate $BaSO_4$) and can affect the surface [6].

Therefore, it is essential to control the surface state of CVCs because it is susceptible to change due to many factors such as sterilization [7,8], preparation procedure before insertion, insertion procedure [9,10], and contact with different media (such as blood [11] and infused drugs [12,13]).

Other solutions than drug solutions, such as locks, can also be in contact with the inner surface of venous catheters. These solutions are used to fill the catheter when not in use to prevent the risk of infections or thrombosis. Some studies have demonstrated that the choice of the lock solution significantly affects the ability of bacteria to adhere to the surface [14].

Ethanol 70% could be used as a lock solution for CVCs. It has shown proven efficiency in reducing catheter-related infection [15–17]. However, the adverse effects on catheters

52 associated with ethanol lock solutions have been reviewed [18]. The observed effects have
53 raised concerns about maintaining the integrity of the catheters after repeated ethanol locks.

54 Unfortunately, only a few studies have examined the impact of ethanol exposure on the
55 mechanical and surface properties of venous catheters [19,20]. In most cases, this impact needs
56 to be described by better comparing different types of polyurethanes.

57 This work focuses on the surface state of polyurethane tubes. It investigates the impact of
58 ethanol 70% on the inner surface properties and the eventual consequences of surface changes
59 on bacterial adhesion. In addition, the biostability concern is discussed by analyzing the
60 migration of antioxidants that protect the polymer chains from degradation.

61

2. Materials and Methods

2.1 Catheters

Four different groups of commercially extruded and sterilized polyurethane tubes with different chemical compositions and barium sulfate loads were used in this study (table 1). The CVC consists of an invasive radio-opaque catheter and a bound extension line (Figure 1). The designation of each type of tube refers to the chemical composition: polycarbonate or polyether nature of the soft segments (PCU or PEU), aliphatic or aromatic structure of the hard segments (Alk or Ar), barium sulfate load w/w- and Shore hardness (XX A or D). All samples were sterilized with ethylene oxide before testing and provided by Vygon.

	Chemical composition	**Shore Hardness**	**Diameters (mm)** d_{int} **X** d_{ext}	**Wall thickness(mm)**	**Barium sulfate load**	**Use**
PCUAr20 80A	Polycarbonate urethane aromatic	80 A	1.05 x 1.65	0.3	20% $BaSO_4$	Catheter
PCUAlk20 95A	Polycarbonate urethane aliphatic	95 A	1.17 x1.67	0.25	20% $BaSO_4$	Catheter
PCUAr40 95A	Polycarbonate urethane aromatic	95 A	1.1x1.67	0.285	40% $BaSO_4$	Experimental
PEUAr 90A	Polyether urethane aromatic	90 A	1.31x 2.08	0.385	-	Extension Line

Table1: Types and specifications of polyurethane tubes used

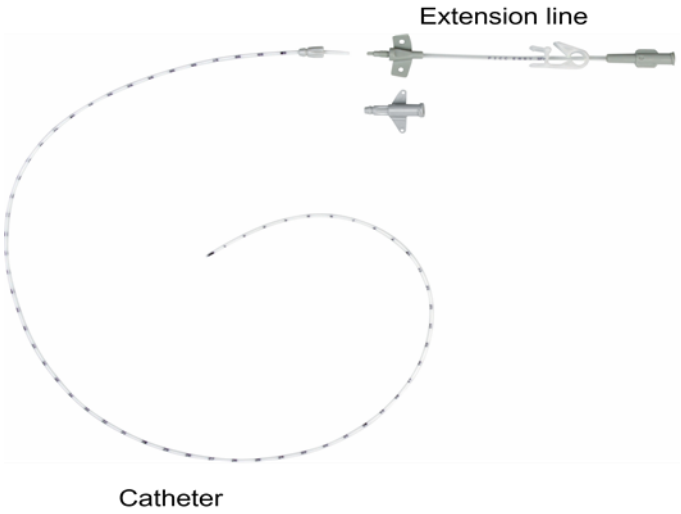

Figure 1: single lumen peripherally inserted central venous catheter

2.2 Samples treatment

All the tubes were treated with EtOH 70% and compared to those, not in contact with any locks or treated with the saline solution for the bacterial adhesion study (control catheters). The type of contact was the lock technique, except for the additive quantification study. Generally, the maximum volume of EtOH lock used to fill the catheter lumen is limited to several µLs. This volume depends on the tube diameters and length. Since some of this quantity is absorbed by the material, restoring the same volume instilled initially in the lumen is impossible. Consequently, it was impossible to conduct a quantitative analysis of leachables under these conditions. The quantitative study of the leachables was thus performed by incubating the tubes in the lock solution and not by instilling the lock into the tube lumen. The (tube surface area) / (lock solution volume) ratio was chosen according to ISO 10993-12. This ratio depends on the shape and thickness of the tested materials: for the tubes, it was equal to 6 cm^2/ml (inner and outer surfaces were in contact and used for this calculation). Compared to the lock conditions, this area/volume ratio corresponds to a worst-case situation.

The duration of contact was 7 days in the case of the ethanol lock. The lock solution was changed daily, and the tubes were rinsed before every new lock instillation and after the last lock instillation using 2 to 3 mL of ultrapure water in a 10 mL syringe. The contact time of 24h

was chosen, as, for several hospital protocols, preconized time contact was between 2 and 24h [21]. Since the locks can be performed several times during the catheter implantation time, the tubes were locked with EtOH seven times.

The temperature was set to 25° or 37° C, depending on the use of the tube. Implanted catheters were stored at 37°C, and extension lines at 25°C.

In order to study the extractables of the polymers, a dissolution (THF)/precipitation (MeOH) process was performed. 2 g of the tube were dissolved using reflux at about 50 °C in 50 mL of tetrahydrofuran (THF). After complete dissolution, the polymer was precipitated by adding an excessive amount of cold methanol; the precipitated polymer was then removed by filtration. The collected solution that contains the extractables was evaporated. After evaporation, the residues were analyzed. Five extractions were made for each type of sample.

2.3 High-performance liquid chromatography (HPLC)

Analyses were performed using an Ultimate 3000 Dionex (Thermo scientific) HPLC system equipped with DAD (diode array detector) and CAD (charged aerosol detector). The system was controlled and monitored by Chromeleon software. Data were acquired and processed with the same software. Separation was achieved on a LiChrospher® 60 RP-select B, 5µm column using three mobile phases. Phases were a mixture of solvents (methanol, acetonitrile, THF, water, and ethyl acetate). A gradient elution consisting of linear gradients from one mobile phase to another was used. The column temperature was set at 30°C thanks to a column oven. The injection volume was 100 µL, and the absorbance was monitored from 220 nm to 400 nm.

The additives were identified by comparing the retention times of pharmaceutical additive standards with the retention times of the peaks found on the chromatogram of the extracted solutions. The quantification was done using points of different concentrations to construct a calibration curve.

2.4 Attenuated total reflection infrared (ATR-FTIR)

The spectrometer apparatus was a PerkinElmer Spectrum Two used in the attenuated total reflection (ATR) mode with a diamond crystal (400–4,000 cm^{-1}). 16 scans were performed with a resolution of 4 cm^{-1}.

30 different spots (on each type of inner tube surface and for each condition) were scanned and averaged.

2.5 Atomic force microscopy (AFM)

The analyses were performed using an Innova AFM (Bruker, Palaiseau, France) in tapping mode with Bruker NCHV-A probes (spring constant 42 N/m – resonance around 320 kHz). The amplitude, phase, and height images were exploited. The scan rate was set at either 0.5 or 1 Hz. At least fifteen areas were scanned. They were randomly distributed on the inner surface of a 2-meter-long tube.

The roughness R_q (root mean squared roughness) and R_a (arithmetic roughness average) were calculated using Gwyddion software.

2.6 Atomic force microscopy (AFM-IR)

An AFM microscope combined with an infrared pulsed tunable laser was used (NanoIR2 from Bruker Nano, CA USA). The spectra (resolution 1 cm^{-1}) were obtained by focusing a multi-chip quantum cascade laser QCL beam (MIRCAT, Daylight solution, CA USA) from the top side of the sample onto the AFM cantilever to perform infrared analysis under the AFM tip. The tunable repetition rate of the source (1 kHz to 500 kHz) was set at the contact resonant frequency of the AFM cantilever. Gold-coated probes were used (MikroMasch: HQ: CSC38/Al-BS-50 - spring constant 0.03 N/m – resonance around 190 kHz).

2.7 Scanning electron microscopy (SEM / EDX)

The inner surface of the tubes was investigated using a FlexSEM 1000 (Hitachi). Two signals were analyzed: the backscattered electrons (BSE) and the secondary electron (SE) signals. The electron beam voltage was set at 2, 10, or 15 kV. No sample preparation was needed. The SEM was coupled with an Oxford energy dispersive spectrometer (EDX), so the device was used to qualitatively analyze the elementary composition on the sample's surface.

2.8 Bacterial Adhesion

Two strains of bacteria were used.

Staphylococcus epidermidis ATCC12228 was chosen to quantitatively assess the bacterial adhesion to the different types of polyurethane tubes.

In addition, a fluorescent strain of *Staphylococcus aureus* RN4220 that expresses GFP protein was also chosen to visualize the bacterial adhesion to the internal surfaces of the tubes. Tryptone Soy Broth medium was used for bacterial cultivation.

Bacterial adhesion assays were performed with cultures harvested and washed three times by 10 minutes centrifugations at 7000 g, and 4 °C. Bacterial pellets were re-suspended in a 0.15 M NaCl medium before use to favor the survival of bacteria. The concentration of the bacterial suspensions was adjusted by measuring the optical density at 400 nm. In order to determine the bacterial suspension concentration, decimal dilutions on 10^6 CFU/mL were carried out, and a count in the mass of a TSA agar medium was carried out for dilutions 10^{-3} and 10^{-4} (1 mL).

About 15 cm long samples of each type of sterile PU tube were locked, either with saline solution (used as a control) or with EtOH 70% for 7 days under aseptic conditions. Before the test, the tubes were drained and rinsed three times with ultra-pure water.

200 µL of bacterial suspension were injected into each tube; the tubes were then clamped and incubated for 2 hours at 37 °C. After adhesion, each tube was rinsed three times in the 0.15 M NaCl medium to remove non-attached or weakly attached bacteria.

In order to proceed to the enumeration of adherent bacteria, the chosen detachment method was to use a very fine sterile swab on the internal surface of the tubes. This method required prior cutting of the tube. The collected adherent bacteria were then detached from the swabs by vigorous shaking (vortex) for 1 min at room temperature in 5 mL NaCl medium. In order to determine the viable and cultivable bacteria number, 1mL of the previous suspension was cultivated in the mass of a TSA agar for 24h. The colonies were counted after 24 hours of incubation at 37 ± 1 ° C, and the number of CFU (Colony Forming Units) per support was calculated. In addition, the inner surfaces of catheters in contact with *S. aureus* were observed under epifluorescence microscopy (Leica DMLB, Leica Microsystems, Nanterre, France) to localize the adherent bacteria. Epifluorescence microscopy also allows seeing if bacteria were adequately removed from the surface after carrying out the different steps of bacterial

detachment. All experiments were completed at least in triplicate and repeated on three different days.

3. Results

3.1 Quantification of the molecules leached in the ethanol lock.

The extractables obtained after the dissolution/precipitation (THF/MeOH) process are very similar to the leachables found in EtOH 70 % incubation solutions and EtOH 70 % lock solutions. However, the extracted amount is more significant, with more intense peaks in the chromatograms (data not shown). Figure 2 shows the chromatograms of the leachables for each PU type incubated in ethanol 70%. It should be emphasized that incubation in EtOH represents a worst-case situation and does not reflect the actual position with EtOH 70% locks due to the substantial difference in the (solution volume)/(tube surface) ratio. However, as the quantification in EtOH 70 % lock condition is not possible, this worst case is used to give a first idea about the possible leaching products and the maximal amount leached in the lock.

Different types of antioxidants are identified as the main extracted component (corresponding to the most significant and highest peak). The good peak separation enables the quantification directly in the solutions. Those antioxidants are mainly primary phenolic antioxidants (maximal absorbance at 280 nm): Irganox 1076 (Octadecyl-3-(3,5-di-tert-butyl-4-hydroxyphenyl)-propionate) and Irganox 1010 (pentaerythritol tetrakis[3-[3,5-di-tert-butyl-4-hydroxyphenyl]propionate) are identified respectively for PEUAr 90A and PCUAr20 80A in chromatograms A and B and for PCUAlk20 95A in chromatogram C. Moreover, a small amount of BHT (butylhydroxytoluene) is observed as a leachable for PEUAr 90A. PCUAr40 95A has no major UV absorbance peak; a smaller peak is observed in the CAD chromatogram that may be attributed to another non-UV-absorbing antioxidant.

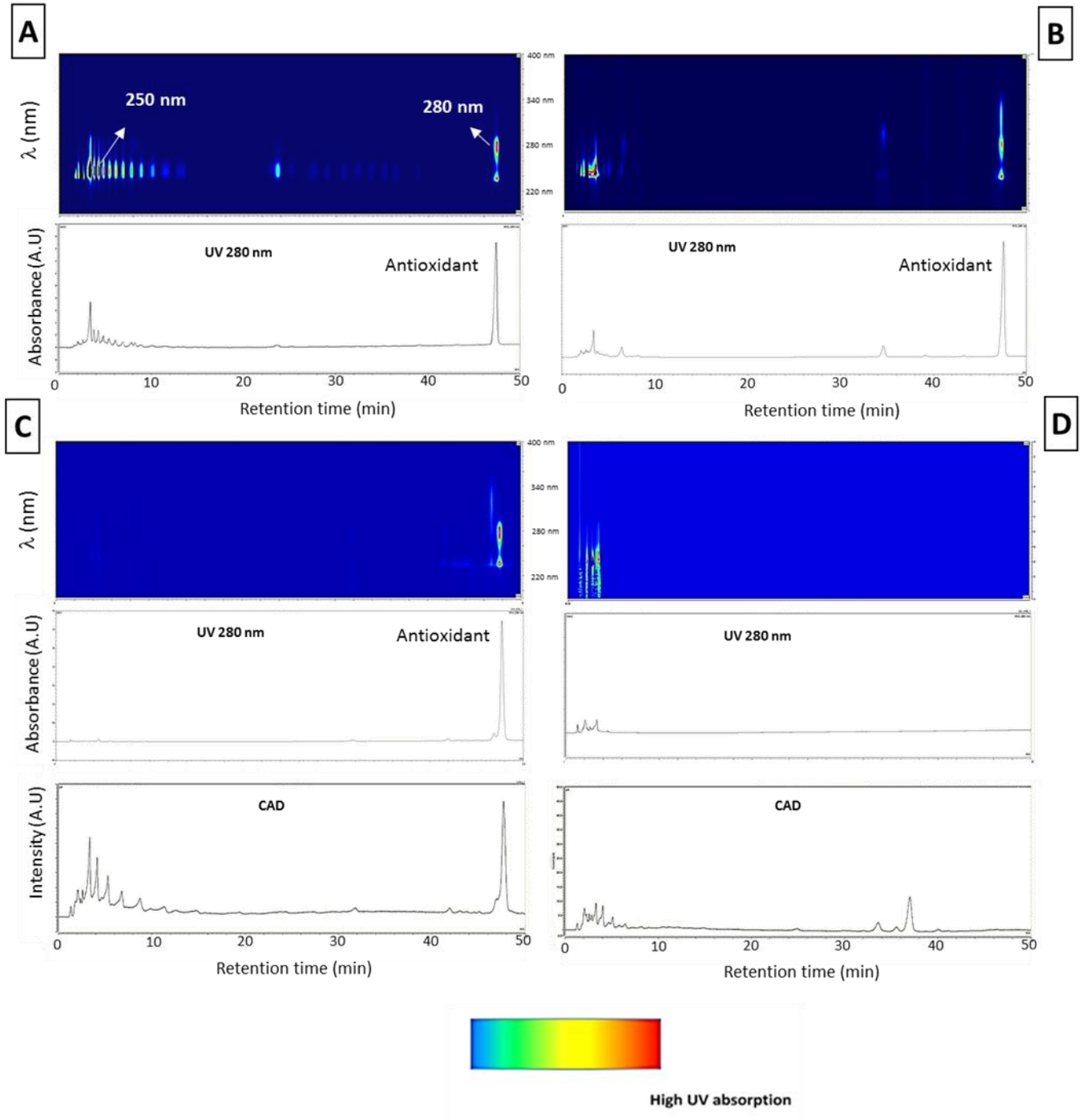

Figure 2: Chromatograms of leachables in ethanol 70% for each PU type for 7 days of contact: DAD 3D chromatograms (time on the x-axis, wavelength on the y-axis, and signal intensity in color), chromatogram at 280 nm and CAD chromatograms for A) PEUAr 90A (DAD detection) B) PCUAr20 80A (DAD detection) C) PCUAlk20 95A (DAD and CAD detection) D) PCUAr40 95A (DAD and CAD detection)

The total phenolic antioxidant content in the control tube is given by the amount of extracted antioxidants and differs depending on the type of catheter. It ranges between 0.3 to 0.5 % (w/w). After 7 days, the ethanol 70 % contains small quantities of the phenolic antioxidants (150 to 180 ppm), representing less than 5% of the total antioxidant estimated content. The most significant loss of antioxidants is noticed for the polyether urethane (table 2)

	Antioxidant type	Total antioxidant estimated content	Antioxidant loss after incubation in EtOH 70% for 7 days
PCUAr20 80A	Irganox 1076	0.54% ± 0.04 (5400ppm ± 400)	148±25 ppm
PCUAlk20 95A	Irganox 1010	0.38% ± 0.02 (3800ppm ± 200)	127±18 ppm
PEUAr 90A	Irganox 1076	0.33% ± 0.01 (3300ppm ± 100)	180± 21 ppm

Table 2: Antioxidant identification and quantification in the initial PU tubes and antioxidant loss after a 7-day ethanol lock. (n =5)

Small quantities of other molecules are leached from the polymer into EtOH 70%. Most of these molecules are probably low molecular weight compounds such as monomers, oligomers, residues from synthesis and sterilization processes, and degradation products. These compounds have proximate retention times suggesting that they may be similar. For the aromatic polyurethane tubes, the absorbance in UV of these compounds is around 250 nm, an absorbance characteristic of aromatic isocyanates. For the aliphatic PCUAlk20 95A, the peaks of these compounds are only visible in the CAD chromatogram and not in the UV chromatogram (non-UV absorbing aliphatic isocyanates). These reasons support the proposition that these molecules can be isocyanate-rich entities (hard segments).

The polyether polyurethane PEUAr 90A shows a more considerable amount and variety of these products leached into EtOH 70%, compared to the other polycarbonate PUs. This significant migration may be due to the higher absorption of ethanol in polyether urethane and

a more significant amount of polymer in the device: the tube walls are indeed thicker than for the other catheters, and there is no inorganic filler.

3.2 Surface chemistry modifications

FTIR-ATR allows the study of the chemical bonds near the material's surface (several µm in depth from the surface). Table 3 shows the general attribution of the different peaks of the spectra. EDX provides the relative amounts of the elements on the surface. In order to calculate the distribution, the spectra of 15 zones of (250*250) µm² are averaged (table 4).

Untreated PU tubes:

The PEUAr 90A spectrum is characterized by certain bands, in particular, the band of H-bonded C=O urethane (1701 cm^{-1}), the C-O ether band (1104 cm^{-1}) and the aromatic ring band (1596 cm^{-1}).

The spectrum of PCUAlk20 95A is characterized by the band of the free C = O carbonate (1739 cm^{-1}), the H bonded C=O urethane (1692 cm^{-1}) band, and the intense band corresponding to the C-O-C bond of the carbonate (1242 cm^{-1}).

PCUAr20 80A and PCUAr40 95A have similar spectra with bands related to the urethane (1079 cm^{-1}), the carbonate (1253 cm^{-1} and 1740 cm^{-1}), and the aromatic ring (1596 cm^{-1}).

Wave number (cm^{-1})	PEUAr	Wave number (cm^{-1})	PCUAr	Wave number (cm^{-1})	PCUAlk
1079	νC-O-C=O (urethane)	1124	νSO4	1124	νSO4
1104	νC-O-C (ether)	1190	νSO4	1190	νSO4
1223	νC-N	1079	νC-O-C=O (urethane)	1079	νC-O-C=O (urethane)
1251	νC-O (sh)	1223	νC-N	1242	νC-O-C (carbonate)
1310	δNH urethane + νC-N	1253	νC-O	1403	δ -CH2
1414	C-C cycle	1310	δNH urethane + νC-N (sh)	1525	δNH urethane + νC-N
1530	δNH urethane + νC-N	1414	C-C cycle	1692	νC=O urethane H bonded
1596	νC=C cycle	1591	νC=C cycle	1740	νC=O Carbonate free
1709	νC=O urethane H bonded	1702	νC=O urethane H bonded	2848	ν (symetric) CH_2
1730	νC=O urethane Free	1740	νC=O Carbonate Free	2915	ν (asymetric) CH_2
2858	ν (symetric) CH_2	2860	ν (symetric) CH_2	3296	νNH H bonded ether
2925	ν (asymetric) CH_2	2920	ν (asymetric) CH_2	3330	νNH H bonded urethane
3296	νNH H bonded ether	3296	νNH H bonded ether		
3330	νNH H bonded urethane	3330	νNH H bonded urethane		

Table 3: Band attribution for the different types of PU tubes

In general, the distribution of the elements is relatively homogenous (EDX results). The surface compositions for the control samples are carbon-rich. The highest carbon ratio is observed for the PEUAr 90A (84 %) and the lowest for the PCUAr40 95A (74%). The oxygen percentage is around 20%, except for the PEUAr 90A (16 %). When the opacifying agent amount increases from 20 to 40 % w/w in the catheters, the barium amount on the surface doubles from 1% to 2%, and the sulfur content also increases (table 4).

	PCUAr20 80A		PCUAlk20 95A		PCUAr40 95A		PEUAr 90A	
	Control	**EtOH lock 7 days**	**Control**	**EtOH lock 7 days**	**Control**	**EtOH lock 7 days**	**Control**	**EtOH lock 7 days**
C (%)	77 ± 0.97	77.7 ± 0.8	78.8 ± 0.71	78.2 ± 0.8	74.7 ± 0.75	74.4 ± 0.9	84.3 ± 1.2	83.9 ± 1.1
O (%)	21 ± 1.2	20.5 ± 0.9	19 ± 0.85	19.5 ± 0.9	21.5 ± 0.9	21.1 ± 0.75	15.6 ± 1.26	16 ± 1.3
S (%)	0.85 ± 0.09	0.9 ± 0.09	1 ± 0.06	1.11 ± 0.08	1.6 ± 0.18	1.8 ± 0.2	-	-
Ba (%)	1.1 ± 0.33	1.05 ± 0.41	1.05 ± 0.09	1.15 ± 0.11	2 ± 0.2	2.2 ± 0.21	-	-

Table 4: The general surface element distribution (atomic percentage) on the catheter surface after a 7-day EtOH lock compared to the control catheter surfaces

After EtOH 70% lock

The contact with the ethanol lock does not significantly impact the element distribution (EDX results) (table 4).

The presence of a lubricant, the ethylene-bis-stearamide (EBS), is more clearly observed on the inner surface, with changes in the absorbance of some FTIR bands corresponding to this lubricant (figure 3): ν NH at 3296 cm^{-1}, ν CH at 2915 and cm^{-1} and amide ν C = O at 1637 cm^{-1} [22]. The band at 1637 cm^{-1} is the most characteristic, since carbonyl stretching bands have a high intensity, and there is no interference with another polyurethane band. Figure 4 represents the absorbance ratio of the band at 1637 cm^{-1} compared to the theoretically unaltered band at 1596 cm^{-1} for the aromatic polyurethanes or the band at 1403 cm^{-1} for the aliphatic one. It indicates that EBS is present at some points of the surface for the non-treated

materials, especially on the PCUAr40 95A surface, and that EBS tends to migrate further to the catheter surface as it is in contact with the ethanol lock. The EBS-enrichment of the surface is relatively low for PEUAr90A (less than 15%) but reaches more than 60% for PCUAR 95A.

Generally, the FTIR-ATR technique allows the investigation of phase separation by studying hydrogen bonding. In addition, it enables the detection of degradation in both the soft and hard polyurethane segments [23,24]. The hydrogen bonds are formed either between two hard segments by linking the carbonyl function of one urethane to the amide function of another urethane or between a soft segment and a hard segment by binding the NH of the urethane to some oxygen (ether or carbonate) from the soft segment [25]. In our case, the presence of additives in the PU tubes does not allow us to detect the changes or reorganization which might happen because of the overlapping with polyurethane bands. Especially the presence of EBS, whose surface concentration changed after the lock and which has IR absorbance in both νN-H and νC = O regions, makes it difficult to assess any change due to chain reorganization. Concerning the soft segment degradation, the decrease in the band at 1104 cm^{-1} and the appearance of a new band at 1174 cm^{-1} in a PEU spectrum is usually attributed to the chain scission of the ether soft segment chains and further cross-linking. The critical band to highlight degradation for the carbonate polyurethanes is the νC-O carbonate band at about 1250 cm^{-1}. None of these changes are detected after locking with EtOH 70% for 7 days.

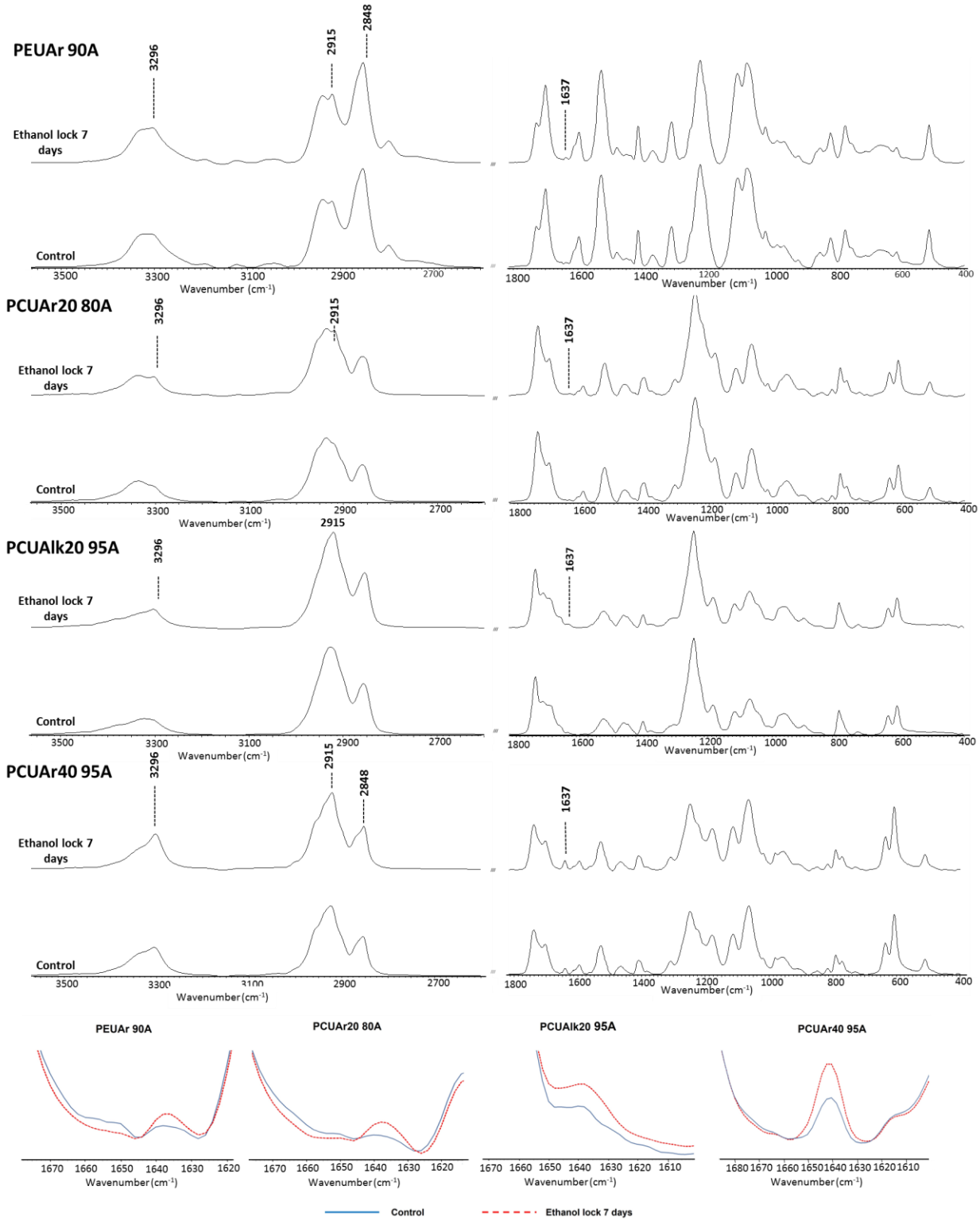

Figure 3: ATR-FTIR spectra of the different PU tubes after a 7-day EtOH lock compared to control spectra

Hard segment degradation is usually highlighted by the absorbance decrease of the bands at 1530 and 1223 cm^{-1} and the concomitant appearance of a new band at 1650 cm^{-1}, which is related to a free aromatic amine. This amine is a product of urethane linkage degradation. These changes are also not detected after contact with EtOH.

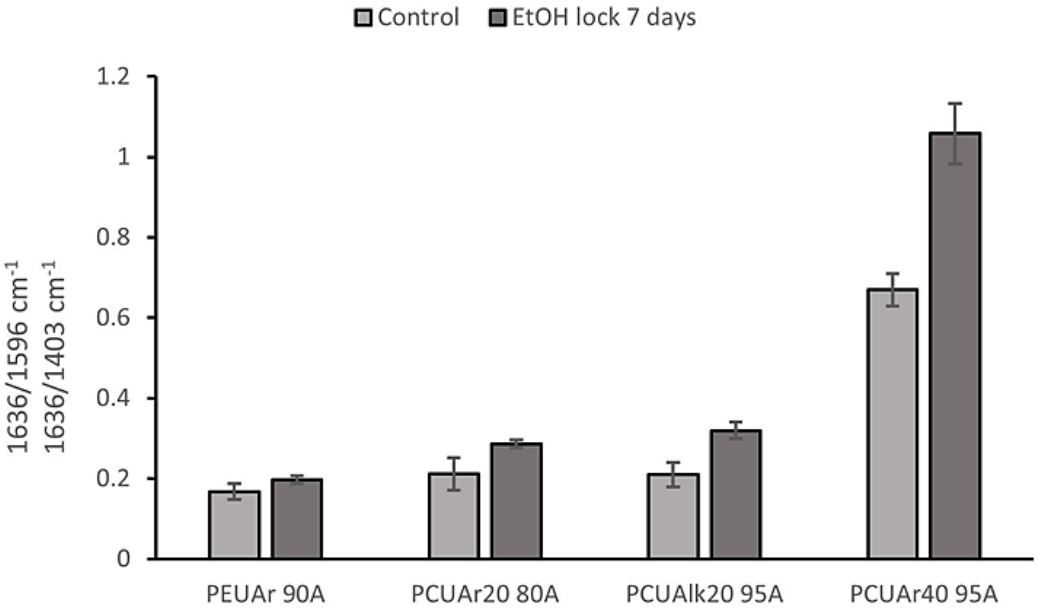

Figure 4: the ratio of band absorbance 1636/1596 cm^{-1} for PEUAr 90A, PCUAr20 80A, and PCUAr40 95A and 1636/1403 cm^{-1} for PCUAlk20 95A after 7 days EtOH lock compared to control catheters

3.3 Surface topography modifications

The topography of the catheters is studied by scanning electron microscopy coupled with energy dispersive x-rays (SEM-EDX) and by atomic force microscopy (AFM).

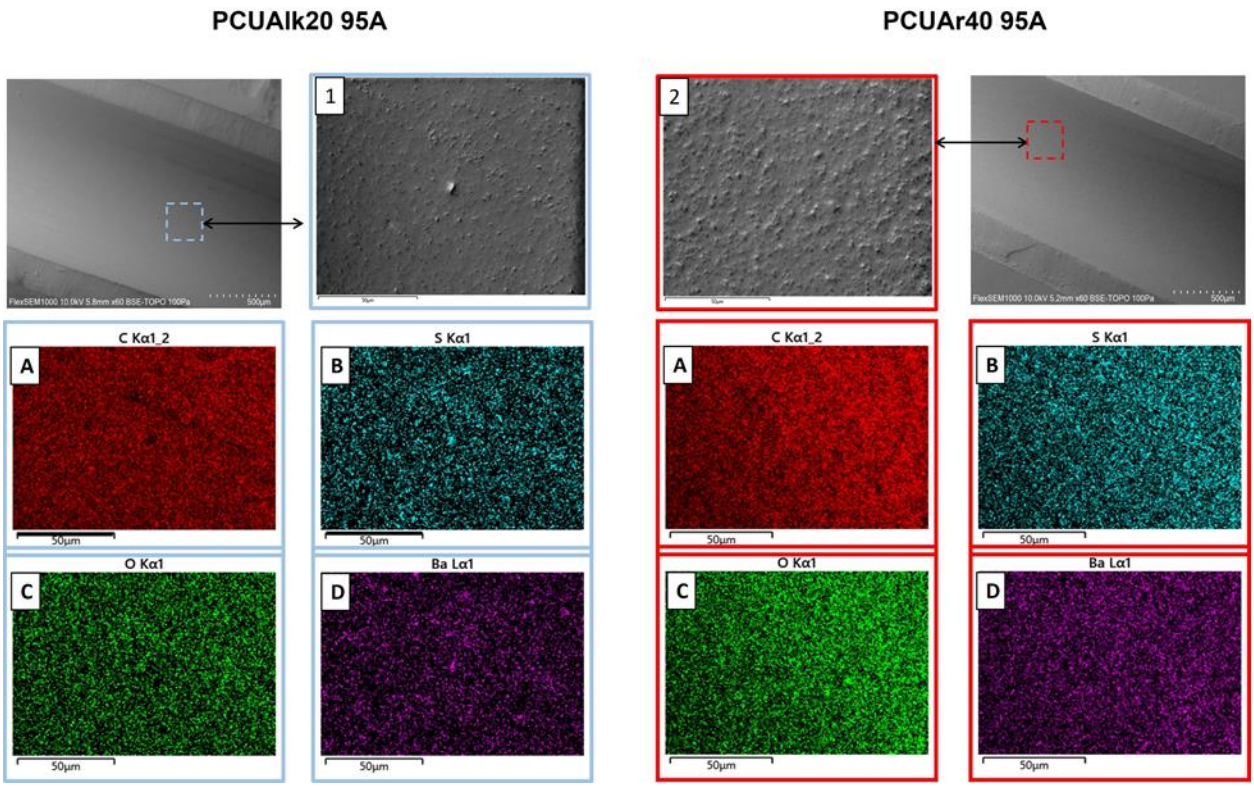

Figure 5: SEM images of untreated PCUAlk20 95A (1) and PCUAr40 95A (2) inner surface (BSE/topographic/ low vacuum mode 100 Pa /10.0kV) showing the general aspects and the granular structure attributed to $BaSO_4$ particles. .Corresponding energy dispersive X-ray (EDX) elemental mapping for C (A), S (B), O (C) and Ba (D) are given.

Control samples:

The inner surface of the control catheter tubes is generally relatively smooth and homogenous. Using the SEM with low magnification shows the presence of parallel striations along the direction of extrusion on the length of the tube (Figure 5). Figure 6 shows the roughness averages R_a and R_q of the four different types of tubes obtained by AFM (n=15) for (20*20), (10*10), and (5*5) μm^2 images. The same trend is observed for all scan sizes. The PCUAr40 95A catheter, which contains the highest ratio of radio-opaque particles, has by far the surface with the highest roughness compared to the other tubes (R_q =128 nm/ R_a =100 nm). On the contrary, the PEUAr 90A tube contains no radio-opaque charge and has a very smooth surface with low roughness. The values for the PCUAr20 80A and PCUAlk20 95A catheters are comparable (R_q = 25-30 nm/ R_a =20-25 nm).

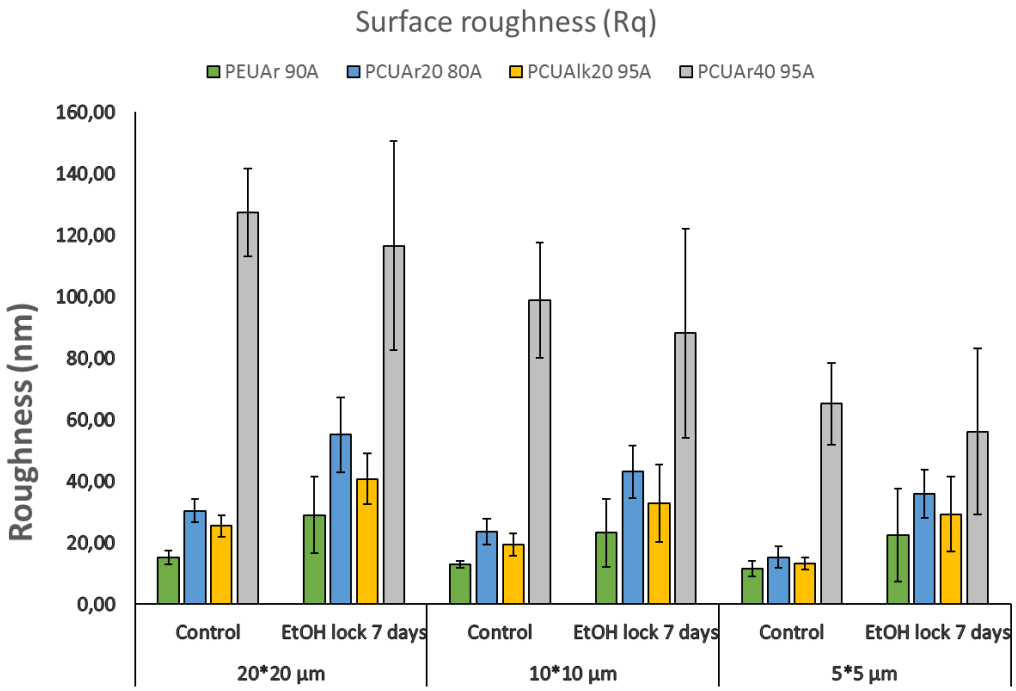

318

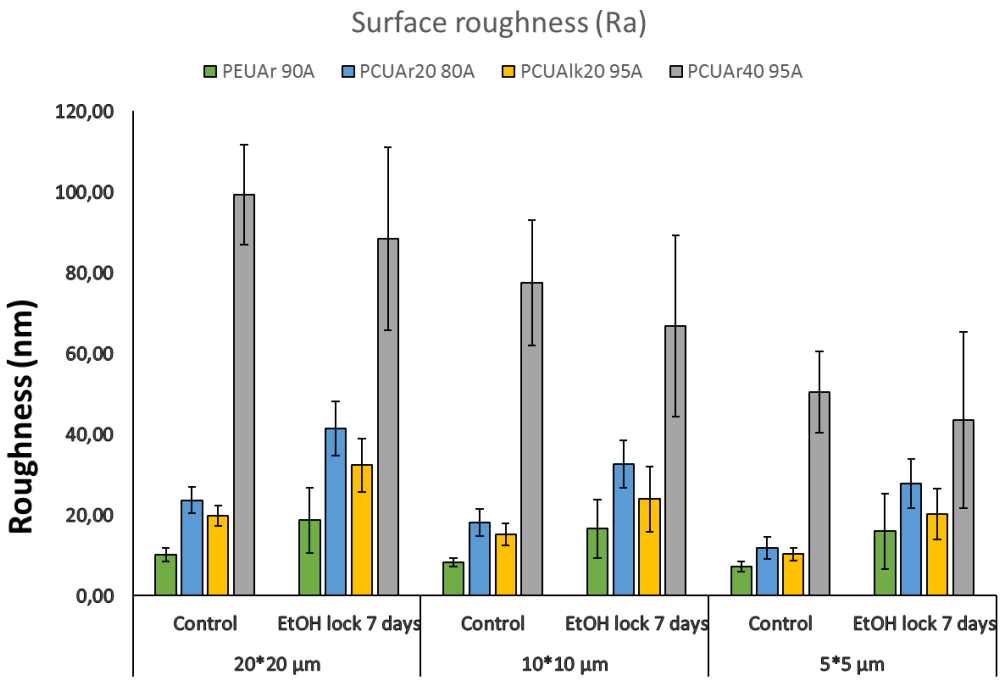

319

320 *Figure 6: Surface roughness (R_q and R_a) of PU tube inner surface after a 7-day EtOH lock compared to control*
321 *catheter surfaces for 20*20, 10*10, and 5*5 μm^2 areas*

322 With higher SEM magnification using secondary electron mode (allowing studying the surface
323 with higher resolution) (figure 7) and with AFM (figure 8), a network of thin protrusions is
324 observed on specific zones of the surface, in addition to the granular structure due to $BaSO_4$

particles (figure 5). These protrusions are thin. The network is regular, expanded, and highly visible on the surface of the PEUAr 90A catheter. It is also visible for PCUAlk20 80A and PCUAlk40 95A but less apparent for the PCUAlk20 95A catheter (see the amplitude images in figure 8). AFM quantifies the size of these surface features: the protrusions' width and height are measured in figure 9. They are a few dozen nanometers high (50-80 nm) and less than 0.5 micrometers wide.

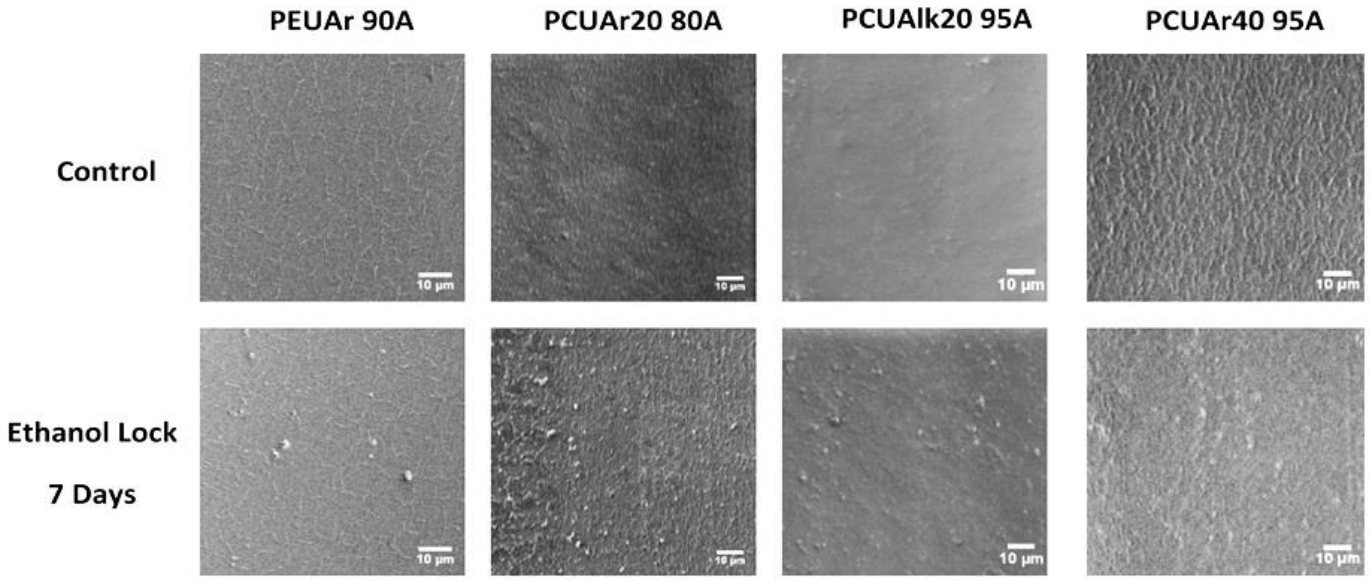

Figure 7: SEM images (SE mode /2.0 kV) of the PU tube inner surface after a 7-day EtOH lock compared to control catheter surfaces. These images show the thin protrusion network structure and the increased number of deposits on the surface after the lock.

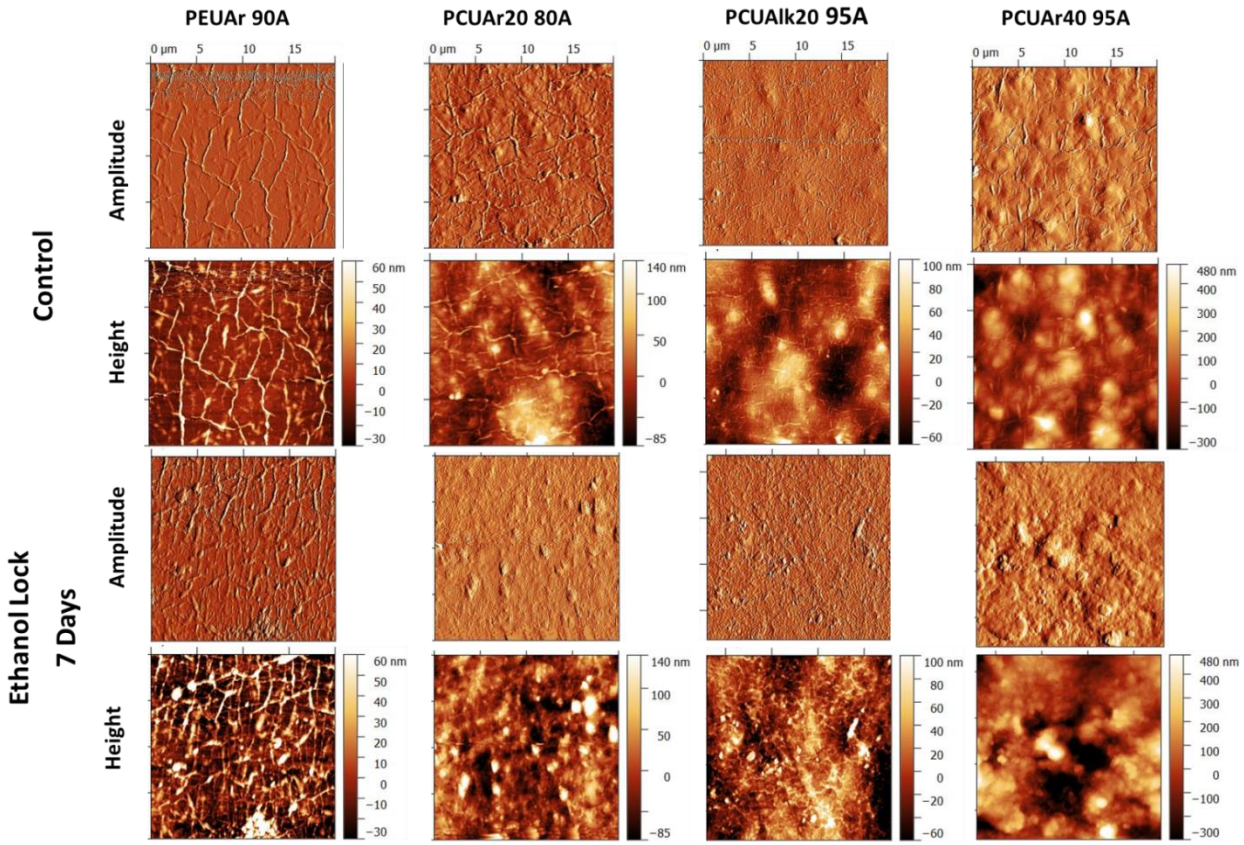

*Figure 8: AFM amplitude and height images (20*20) µm² of PU tubes inner surfaces after a 7-day EtOH lock compared to control catheter surfaces*

High spots up to hundreds of nanometers are observed on the AFM images of the radio-opaque catheter surface (figure 8). The width of these spots is 1-2 µm for the PCUAr20 80A and PCUAlk20 95A catheters and up to 4 µm for the PCUAr40 95A catheters (Figure 9). In order to better understand the chemistry of the tubes' inner surface, an AFM-IR analysis is performed. This technique combines the topographic study with the nanoscale spectroscopic analysis [26,27]. The images are relatively similar to those obtained in tapping mode. The IR spectrum is performed at selected points of interest. For example, in Figure 10 A, the spectrum corresponding to the high spot is characteristic of a barium sulfate-rich area as the bands at 1124, and 1200 cm^{-1} are higher compared to the background polymer spectrum, which is characterized by the bands in the C = O absorbance region (1700-1740 cm^{-1}).

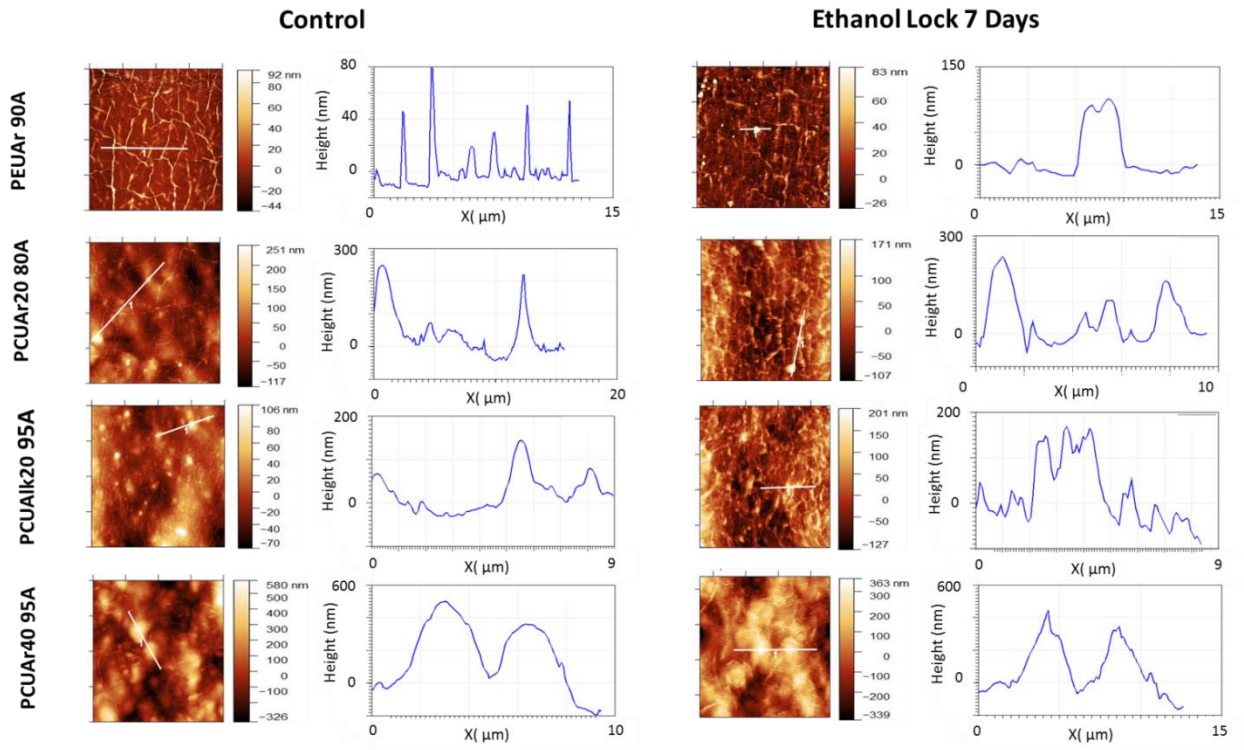

Figure 9: AFM height images and profiles of PU tube inner surface after a 7-day EtOH lock compared to control catheter surfaces (the profiles correspond to the white line on the AFM images)

The same approach is used to carry out a surface mapping using the 1124 ($BaSO_4$) and 1740 cm^{-1} (PU) absorption bands (Figure 10 C, D); 1740 cm^{-1} lower absorbance and 1124 cm^{-1} higher absorbance regions are overlaid and match the high points previously observed on the height images (figure 10 B). It confirms that these points are due to the presence of the $BaSO_4$ particles.

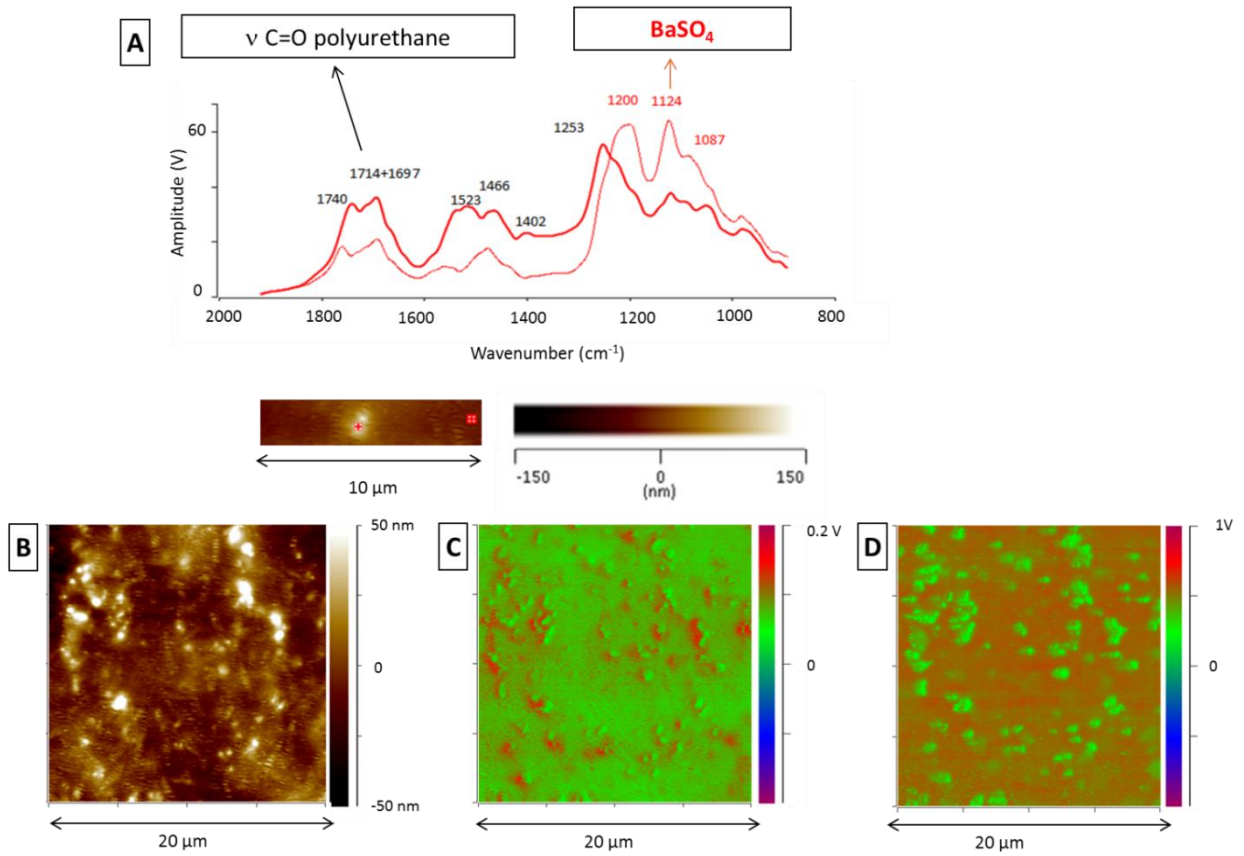

Figure 10: A) IR spectrum of a high spot observed on the height image below and attributed to a $BaSO_4$ particle (thin line) compared to a spectrum characteristic of the rest of the PCUAlk20 95A inner surface (bold line) B) 20X20 mm^2 height image of the inner surface of PCUAlk20 95A tube C) mapping at 1124 cm^{-1} band absorbance for the same area and D) mapping at 1740 cm^{-1} band absorbance for the same area.

After 7 days of ethanol 70 % locking, the inner surface of the tubes remains intact: no cracks, notches, nor pits are observed by SEM (figure 7).

The surface texture is not much impacted. The most noticeable change is the increasing number of small deposits or particles on the surface for all types of PU catheters (figure 7 and figure 8). Comparing control to ethanol-locked samples, the surface of the PEUAr 90A seems to be the most impacted by these deposits because its initial very smooth surface becomes less homogenous with the appearance of some spots (1 micron wide and around 100 nm high, as shown by figure 9). For the radiopaque tubes, some changes in the distribution of the higher points occur with the beginning of an aggregation phenomenon on 10-20 µm zones (figure 11). By examining the tube surface with energy-dispersive X-ray (EDX) analysis used in conjunction

with SEM, those aggregations are attributed to $BaSO_4$ (figure 11). The thin protrusion network is less clearly visible on some areas of the inner surface of radiopaque catheters (figure 8).

Concerning the surface roughness, the dispersion of the results increases strongly after the lock (+30-35%), indicating a more heterogeneous surface after the ethanol lock. For PCUAr4095A, the roughness decreases on average for all the scan sizes, even if the differences between the roughness values are not statistically significant (figure 6). The opposite trend is observed for the other tubes.

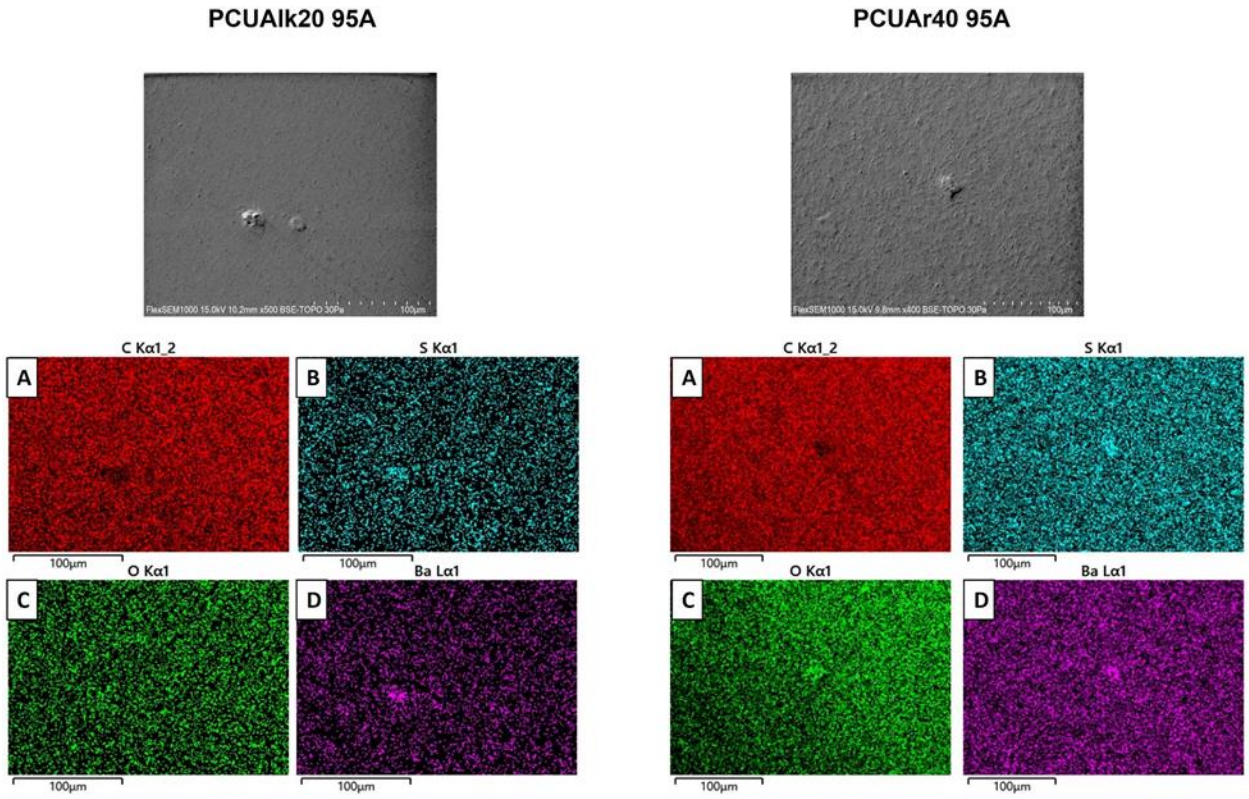

Figure 11: SEM images of PCUAlk20 95A and PCUAr40 95A inner surface after locking 7 days with EtOH (BSE/topographic mode/ low vacuum mode 30 Pa /15.kKV) showing the aggregation of the $BaSO_4$. Corresponding energy dispersive X-ray (EDX) elemental mapping for C (A), S (B), O (C) and Ba (D) are given

3.4 Bacterial adhesion

Studying bacterial adhesion to the central catheter surface is essential, as adhesion is crucial in initiating colonization and subsequent infection. Any change in the surface properties can modify the bacterial adhesion on the catheter surface.

S.epidermidis and *S.aureus* were chosen to study the bacterial adhesion to the inner surface of the different types of polyurethane tubes before and after the EtOH lock because coagulase-negative strains (C-NS), especially *S.epidermidis* [28] and *S.aureus,* are the most common pathogens causing hospital bloodstream infections [29].

The observed bacterial adhesion pattern is made up of clusters or aggregations of bacteria. Some areas of the PCUAr40 95A inner surface exhibit particular adhesion morphologies: the bacteria follow a specific branched pattern on the surface (Figure 12).

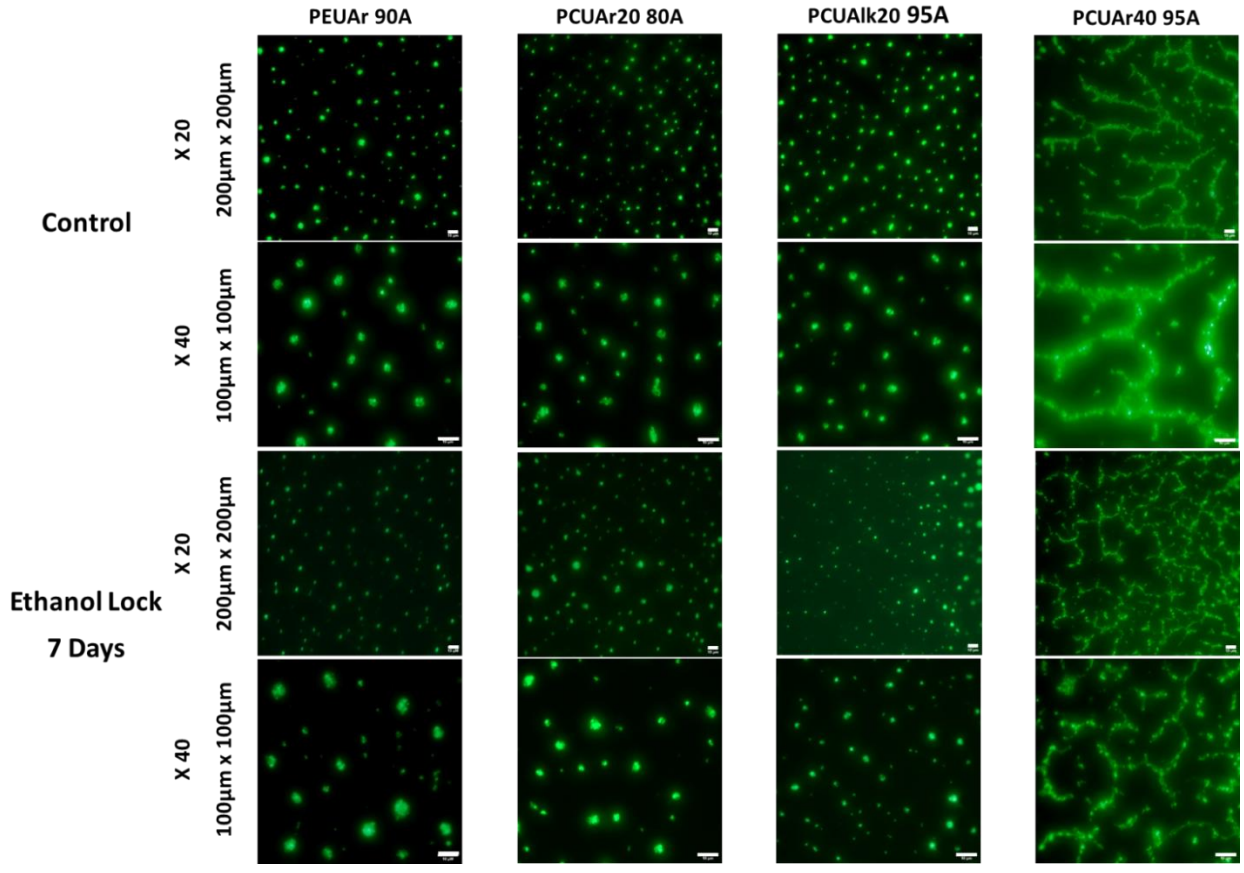

Figure 12: fluorescent images of S.aureus adhesion on the inner surfaces of PU tubes after a 7-day EtOH lock compared to control catheter surfaces (the scale bar in white is 10 µm for all images)

The tests were carried out with 10^7, 10^8, and 10^9 CFU/mL bacterial suspensions of *S. aureus*. As the concentration increases, this branched pattern appears on the other tubes, but to a lesser extent for PEUAr 90A (Figure 13).

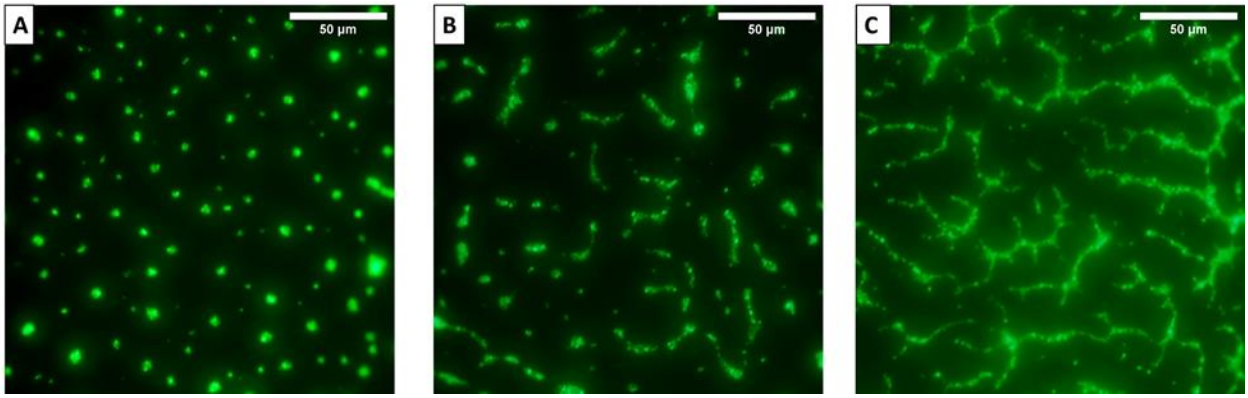

Figure 13: fluorescent images of S.aureus showing the evolution of bacterial adhesion on the inner surface of PCUAlk20 95A A) 10^7B) 10^8 C) 10^9 CFU/mL suspension (the scale bar in white is 50 µm for all images)

As mentioned in Materials and Methods, the detachment method uses a very fine swab and requires prior catheter cutting to proceed to the enumeration of adherent bacteria. The cutting and the swab friction may impact the results a little, but few bacteria remain on the inner surface except those trapped in the extrusion striations described before (Figure 14).

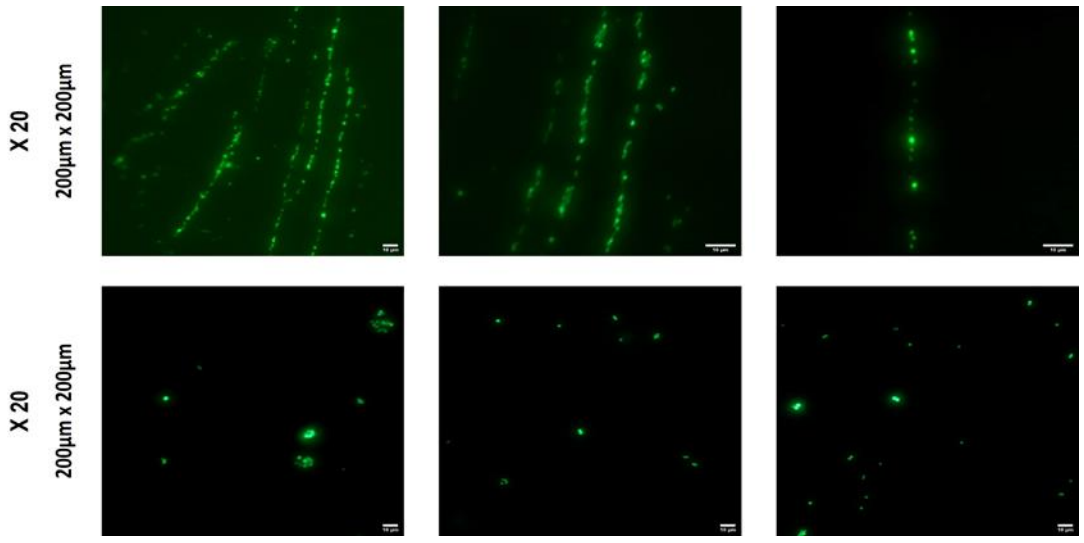

Figure 14: fluorescent images of remaining S.aureus after detachment from the surface of PCUAr40 95A control samples (the scale bar in white is 10 µm for all images)

Regarding the number of bacteria counted, the PEUAr 90A surface shows the lowest bacterial adhesion. In contrast, the PCUAr40 95A surface, which contains the highest level of $BaSO_4$,

shows the highest with a difference of about 0.5 log. No significant difference is observed between the aromatic and aliphatic polyurethanes.

After the ethanol lock, changes in bacterial adhesion to the inner surface occur. *S. epidermidis* adheres slightly higher to the ethanol-treated PU, but this difference is small and insignificant to impact the clinical level. The most substantial effect is observed for the PCUAr40 95A catheter (Figure 15).

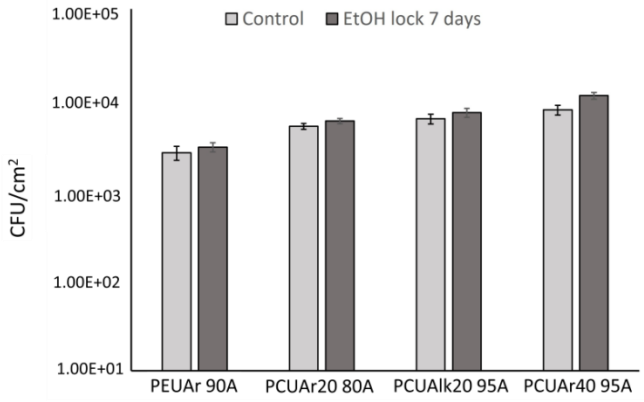

	Population ratio of bacteria: EtOH treated / Control
PEUAr 90A	1.15
PCUAr20 80A	1.15
PCUAlk20 95A	1.17
PCUAr40 95A	1.45

Figure 15: Bacterial adhesion (S. epidermidis) on the inner surface of PU tubes expressed in CFU/cm² and population ratio of bacteria after a 7-day EtOH lock compared to control catheters

4. Discussion

This work investigated the possible impact of EtOH lock 70% on the inner surface of different polyurethane tubes after 7 days of contact.

Overall, after 7 days of ethanol lock, the results showed that the surface of all polyurethane tubes did not present any remarkable evidence of degradation in soft or hard segments, as shown by the FTIR-ATR results and by the AFM and SEM images.

On the other hand, the polymeric material of the tubes was able to absorb ethanol at different rates and ratios, depending on the chemical nature of the polymer. As shown by the results of liquid chromatography, this absorption promoted the extraction of small quantities of low molecular weight compounds from the bulk and the surface of the tubes. These molecules consisted in part of residues of synthesis, oligomers, and degradation products. Most of these molecules had a

maximum absorbance of 250 nm for aromatic polyurethane. They were not visible on the UV chromatogram of the aliphatic PUs, suggesting they were isocyanate-rich products. The results were consistent with previous studies, which focused on the leaching of compounds from extruded polyurethane catheters, as these catheters were in contact with alcohol. These studies have demonstrated that these leached compounds were additives (such as antioxidants) and hard segment-rich oligomers [30]. Yokoama et al. [31] have detected a polyurethane chain extender (1,4-butanediol) in ethanol after catheter immersion 24h in ethanol or after dynamic infusion conditions (30ml/h for 24h). In this last case, the chain extender release was about 130 µg. Msakni et al. have shown that products tend to migrate faster and to a greater extent with a higher concentration of ethanol [32]. They have demonstrated that for carbothane polyurethane immersed in 95% ethanol, the release of leachables at 37°C was quick and primarily occurred in the first 4 hours of contact. However, the leachable amount was minimal for lower ethanol percentage (40%) and shorter contact time. So, because of the possible toxicity of the leached products, they have suggested that a lock of 30 min with 40 % EtOH was safe and effective in preventing infectious complications. Our results suggest also aspirating the EtOH lock after the contact period and rinsing the tubes is recommended.

Under our study conditions, EtOH extracted antioxidants. These antioxidants are added to the polymer to protect it from the oxidative environment. By performing a worst case (total immersion of the tube), the antioxidant loss was 3-5% after 7 repeated days of ethanol locking. This low loss will have a minor impact on the oxidation of the tubes. However, repeated locks or locks for more prolonged periods might lead to higher migrations.

Ethylene bis stearamide (EBS) migration to the surface is another consequence of ethanol contact. EBS has a hydrophobic nature, and its migration may lead to more hydrophobic surfaces of polyurethane tubes.

The dimensions, the chemical structure, and the organization of the topographical features influence the surface properties such as roughness and hydrophobicity. In our case, the surface features were nanostructured with thin protrusion networks. However, microscale structures

were also present, such as the high spots related to $BaSO_4$ particles for the radio-opaque tubes. These $BaSO_4$ particles increased the surface roughness significantly. The higher the $BaSO_4$ percentage, the higher the roughness. The contact with the ethanol lock increased the irregularities of the inner surface of the PU tubes. The roughness increased for the EtOH-locked tube, and the surface became less homogenous. Due to the extraction power of EtOH, the number of deposits on the surface increased, as supported by the observation of the EBS exudation and other compounds' leaching. The structure of the surface became less uniform, maybe due to other factors, such as the mechanical stress resulting from the successive absorption and desorption processes of ethanol and the modified distribution of the $BaSO_4$ particles (tendency to merge). In addition, as the exudation of EBS was particularly strong in the case of PCUAr95A, it could explain, conjointly to a more substantial aggregation phenomenon (more particles initially for this tube), the texture modification observed (the roughness is reduced compared to the control sample). However, we did not highlight any damage to the inner surface as observed previously in the case of ethanol contained in etoposide formulation (ratio around 30%). In this case, Yokohama et al. have noticed [33] that after 24 hours of infusion, cracking of the inner wall and spot-like melting occurred. The study of Msakni et al. [32] has shown that increasing the ethanol content and the contact time increased the surface degradation with the apparition of flake structures. However, they have not highlighted the appearance of any cracks. Their control surface was granular, but the origin of this granular structure has not been discussed (no information on the presence of any radio-opaque agent in their carbothane catheter). After contact, the granular structure disappeared, and flakes appeared. No modification was observed for short times and low ethanol content (30 min 40% EtOH). Modifications were perceptible after 4 h and for EtOH contents higher than 60%.

The bacterial adhesion was assessed to detect any alteration after EtOH locking. For other locks, such as heparin, it has been shown that the lock promoted biofilm formation [34]. Instillating EtOH is known to reduce the infectious risk for the patient. However, as it modified the surface features, the ability of bacteria to adhere to a catheter surface can change (positively or negatively) between two locks. Several physicochemical and topographical factors, such as surface energy, electrostatic charge, and hydrophobicity, influence this ability.

[3,35,36]. In most cases, the positive surface charge effectively promotes bacterial adhesion (positive surface charge attracts the negative charge of most bacteria). The effect of roughness on adhesion is much more complex. Mean roughness values such as R_q or R_a are not always relevant factors regarding bacterial adhesion because identical values can correspond to surfaces with very different textures and configurations. The ability of the bacteria to colonize a surface depends on the shape and the scale of the surface features: an increase in roughness can, for example, limit the effect of rinsing as the bacteria are trapped and protected by the roughness, and it can offer to the bacteria a higher surface area to adhere. For instance, the detachment of $BaSO_4$ particles from the surface of hemodialysis catheters creates holes on the surface that promote bacterial proliferation [6]. However, asperities at a smaller scale than the bacterium can limit the adhesion force to the surface by limiting the contact between the bacterium surface and the material surface [37]; it can even cause cell death in the case of very sharp nanopillars on the surface [38].

The presence of the hydrophobic EBS at some areas of the surface, the amount of electrostatic charge brought to the surface by $BaSO_4$, and the surface roughness and heterogeneity that conform or not to the bacterial shape may alter the homogenous distribution of the bacteria at the surface. All these factors were more accentuated for the PCUAr40 95A catheter, which exhibited a higher $BaSO_4$ ratio and a greater EBS exudation. These accentuated factors might explain the exhibition of a particular pattern of bacteria distribution on the PCUAr40 95A surface, even for the lower bacterial suspension concentrations. The 7-day ethanol lock resulted in surface topography modifications and increased the surface hydrophobicity because of further EBS exudation. However, it did not significantly affect the initial bacterial adhesion: the little increase in the CFU on the surface of the treated catheter was statistically significant, but the increase, which was less than 1 log, was not “microbiologically” relevant. It should be noted that a higher adhesion increase occurred for the PCUAr40 95A, which had the strongest ethanol-promoted EBS exudation. In the future, it should be checked that the observed surface changes do not promote biofilm formation and growth.

Conclusion

The surface state of polyurethane catheter tubes depends on the catheter composition, the polymer additives, the manufacturing processes (extrusion and sterilization), and the storage conditions. Especially the presence of the $BaSO_4$radiopaque agent particles highly impacts the surface roughness.

Although EtOH lock does not cause any critical degradation of the polymer material resulting in cracks or pits on the surface, locking with EtOH 70% for 7 days impacts the surface properties of polyurethane catheters. The EtOH extracts low molecular weight products from polyurethane and favors the migration of additives to the surface. A radio-opaque $BaSO_4$ particle aggregation tendency also occurs after locking with EtOH.

Though, these modifications have a low and insignificant impact on bacterial adhesion on the inner surface. So EtOH is not only an efficient antibacterial agent, it does not promote any higher risk of promoting bacterial adhesion and so infections between two locks.

Acknowledgments

Afif Khzam was supported by a CIFRE doctoral fellowship funded by ANRT on behalf of the French Ministry of Research with a partnership with Vygon company.

Data availability statement

Supporting data is not available.

References

[1] J.F. Hecker, L.A. Scandrett, Roughness and thrombogenicity of the outer surfaces of intravascular catheters, Journal of Biomedical Materials Research. 19 (1985) 381–395. https://doi.org/10.1002/jbm.820190404.

[2] G.H. Nachnani, L.S. Lessin, T. Motomiya, W.N. Jensen, Scanning Electron Microscopy of Thrombogenesis on Vascular Catheter Surfaces, New England Journal of Medicine. 286 (1972) 139–140. https://doi.org/10.1056/NEJM197201202860306.

[3] S.E. Tebbs, A. Sawyer, T.S.J. Elliott, Influence of surface morphology on in vitro bacterial adherence to central venous catheters, British Journal of Anaesthesia. 72 (1994) 587–591. https://doi.org/10.1093/bja/72.5.587.

[4] M. Nouman, E. Jubeli, J. Saunier, N. Yagoubi, Exudation of additives to the surface of medical devices: impact on biocompatibility in the case of polyurethane used in implantable catheters, Journal of Biomedical Materials Research Part A. 104 (2016) 2954–2967. https://doi.org/10.1002/jbm.a.35837.

[5] B.J. Tyler, BD. Ratner, D.G. Castner, D. Briggs, Variations between Biomer^{TM} lots. I. Significant differences in the surface chemistry of two lots of a commercial poly(ether urethane), Journal of Biomedical Materials Research. 26 (1992) 273–289. https://doi.org/10.1002/jbm.820260302.

[6] F. Verbeke, U. Haug, A. Dhondt, W. Beck, A. Schnell, R. Dietrich, R. Deppisch, R. Vanholder, The role of polymer surface degradation and barium sulphate release in the pathogenesis of catheter-related infection, Nephrol Dial Transplant. 25 (2010) 1207–1213. https://doi.org/10.1093/ndt/gfp638.

[7] O. Mrad, J. Saunier, C. Aymes-Chodur, V. Rosilio, S. Bouttier, F. Agnely, P. Aubert, J. Vigneron, A. Etcheberry, N. Yagoubi, A Multiscale Approach to Assess the Complex Surface of Polyurethane Catheters and the Effects of a New Plasma Decontamination Treatment on the Surface Properties, Microscopy and Microanalysis. 16 (2010) 764–778. https://doi.org/10.1017/S1431927610093876.

[8] M. Nouman, J. Saunier, E. Jubeli, C. Marlière, N. Yagoubi, Impact of sterilization and oxidation processes on the additive blooming observed on the surface of polyurethane, European Polymer Journal. 90 (2017) 37–53. https://doi.org/10.1016/j.eurpolymj.2017.03.002.

[9] B. Parvez, N. Parmar, A.K.C. Chan, Trimming of peripherally inserted central venous catheters may increase the risk of thrombosis, Thrombosis Research. 113 (2004) 175–177. https://doi.org/10.1016/j.thromres.2004.02.013.

[10] A. Jegatheeswaran, N. Parmar, J.M. Walton, C. Yip, A.K. Chan, Quantitative analysis of catheter roughness induced by cutting and manipulation: a potential prothrombotic risk, Blood Coagulation & Fibrinolysis. 18 (2007) 531–536. https://doi.org/10.1097/MBC.0b013e3282010ae6.

[11] G. Gunaratnam, C. Spengler, S. Trautmann, P. Jung, J. Mischo, B. Wieland, C. Metz, S.L. Becker, M. Hannig, K. Jacobs, M. Bischoff, Human blood plasma factors affect the adhesion kinetics of Staphylococcus aureus to central venous catheters, Sci Rep. 10 (2020) 20992. https://doi.org/10.1038/s41598-020-77168-x.

[12] U. Braun, E. Lorenz, C. Weimann, H. Sturm, I. Karimov, J. Ettl, R. Meier, W.A. Wohlgemuth, H. Berger, M. Wildgruber, Mechanic and surface properties of central-venous port catheters after removal: A comparison of polyurethane and silicon rubber materials, Journal of the Mechanical Behavior of Biomedical Materials. 64 (2016) 281–291. https://doi.org/10.1016/j.jmbbm.2016.08.002.
[13] E. Tabone, J.F. Latour, A. Mignot, J.Y. Rauchere, Alteration of the inner surface of venous catheters by antineoplastic drugs, Biomaterials. 12 (1991) 741–746. https://doi.org/10.1016/0142-9612(91)90023-4.
[14] R.M.Q. Shanks, J.L. Sargent, R.M. Martinez, M.L. Graber, G.A. O'Toole, Catheter lock solutions influence staphylococcal biofilm formation on abiotic surfaces, Nephrology Dialysis Transplantation. 21 (2006) 2247–2255. https://doi.org/10.1093/ndt/gfl170.
[15] R.J. Sherertz, M.S. Boger, C.A. Collins, L. Mason, I.I. Raad, Comparative In Vitro Efficacies of Various Catheter Lock Solutions, Antimicrobial Agents and Chemotherapy. 50 (2006) 1865–1868. https://doi.org/10.1128/AAC.50.5.1865-1868.2006.
[16] J. Zhang, B. Wang, J. Wang, Q. Yang, Ethanol locks for the prevention of catheter-related infection in patients with central venous catheter: A systematic review and meta-analysis of randomized controlled trials, PLoS One. 14 (2019) e0222408. https://doi.org/10.1371/journal.pone.0222408.
[17] K.P. Pieroni, C. Nespor, M. Ng, M. Garcia, M. Hurwitz, W.E. Berquist, J.A. Kerner, Evaluation of Ethanol Lock Therapy in Pediatric Patients on Long-Term Parenteral Nutrition, Nutrition in Clinical Practice. 28 (2013) 226–231. https://doi.org/10.1177/0884533612468009.
[18] L.A. Mermel, N. Alang, Adverse effects associated with ethanol catheter lock solutions: a systematic review, Journal of Antimicrobial Chemotherapy. 69 (2014) 2611–2619. https://doi.org/10.1093/jac/dku182.
[19] CJ Crnich, J.A. Halfmann, W.C. Crone, D.G. Maki, The Effects of Prolonged Ethanol Exposure on the Mechanical Properties of Polyurethane and Silicone Catheters Used for Intravascular Access, Infection Control & Hospital Epidemiology. 26 (2005) 708–714. https://doi.org/10.1086/502607.
[20] G.J. McHugh, D.J.C. Wild, J.H. Havill, Polyurethane Central Venous Catheters, Hydrochloric Acid and 70% Ethanol: A Safety Evaluation, Anaesth Intensive Care. 25 (1997) 350–353. https://doi.org/10.1177/0310057X9702500404.
[21] EtOH-lock_ADULT.pdf, (n.d.). https://www.med.umich.edu/asp/pdf/adult_guidelines/EtOH-lock_ADULT.pdf (accessed May 16, 2022).
[22] A. Sawyer, J. Bandekar, H. Li, Examination of wax on surface of extruded Pellethane by scanning electron microscopy attenuated total reflection-infrared and x-ray photoelectron spectroscopy and its importance in blood compatibility, Journal of Vacuum Science & Technology A. 12 (1994) 2966–2970. https://doi.org/10.1116/1.578923.
[23] E.M. Christenson, J.M. Anderson, A. Hiltner, Oxidative mechanisms of poly(carbonate urethane) and poly(ether urethane) biodegradation: In vivo and in vitro correlations, Journal of Biomedical Materials Research Part A. 70A (2004) 245–255. https://doi.org/10.1002/jbm.a.30067.

[24] E.M. Christenson, M. Dadsetan, M. Wiggins, J.M. Anderson, A. Hiltner, Poly(carbonate urethane) and poly(ether urethane) biodegradation: In vivo studies, Journal of Biomedical Materials Research Part A. 69A (2004) 407–416. https://doi.org/10.1002/jbm.a.30002.
[25] C.D. Eisenbach, W. Gronski, Hydrogen bonding and phase separation in segmented polyurethane elastomers as studied by 13C NMR magic angle spinning and FT-IR spectroscopy, Die Makromolekulare Chemie, Rapid Communications. 4 (1983) 707–713. https://doi.org/10.1002/marc.1983.030041103.
[26] J. Mathurin, A. Deniset-Besseau, D. Bazin, E. Dartois, M. Wagner, A. Dazzi, Photothermal AFM-IR spectroscopy and imaging: Status, challenges, and trends, Journal of Applied Physics. 131 (2022) 010901. https://doi.org/10.1063/5.0063902.
[27] A. Dazzi, C.B. Prater, AFM-IR: Technology and Applications in Nanoscale Infrared Spectroscopy and Chemical Imaging, Chem. Rev. 117 (2017) 5146–5173. https://doi.org/10.1021/acs.chemrev.6b00448.
[28] M.A. Martin, M.A. Pfaller, R.P. Wenzel, Coagulase-Negative Staphylococcal Bacteremia, Ann Intern Med. 110 (1989) 9–16. https://doi.org/10.7326/0003-4819-110-1-9.
[29] M.B. Edmond, S.E. Wallace, D.K. McClish, M.A. Pfaller, R.N. Jones, R.P. Wenzel, Nosocomial Bloodstream Infections in United States Hospitals: A Three-Year Analysis, Clinical Infectious Diseases. 29 (1999) 239–244. https://doi.org/10.1086/520192.
[30] M. Renier, Y.K. Wu, J.M. Anderson, A. Hiltner, G.A. Lodoen, C.R. Payet, Characterization of extractable species from poly(etherurethane urea) (PEUU) elastomers, Journal of Biomaterials Science, Polymer Edition. 5 (1994) 511–529. https://doi.org/10.1163/156856294X00185.
[31] H. Yokoyama, T. Aoyama, K. Nakajima, Y. Yamada, H. Sato, S. Chiba, H. Hirai, T. Iga, [Investigation of the cause of polyurethane catheter cracking during constant infusion of etoposide (VP-16) injection (2)--Analysis of ethanol eluting materials from catheter], Yakugaku Zasshi. 123 (2003) 799–803. https://doi.org/10.1248/yakushi.123.799.
[32] N. Msakni, M.-J. Galmier, M.-J. Couret, C. Szczepaniak, B. Bouchon, B. Souweine, C. Lartigue, Complementary mass spectrometric approaches and scanning electron microscopy to study the structural stability of polyurethane tunneled dialysis catheters after exposure to ethanol solutions, Rapid Communications in Mass Spectrometry. 27 (2013) 2343–2354. https://doi.org/10.1002/rcm.6691.
[33] H. Yokoyama, T. Aoyama, T. Matsuyama, Y. Yamamura, K. Nakajima, K. Nakamura, H. Sato, H. Kotaki, S. Chiba, H. Hirai, Y. Yazaki, T. Iga, [The cause of polyurethane catheter cracking during constant infusion of etoposide (VP-16) injection], Yakugaku Zasshi. 118 (1998) 581–588. https://doi.org/10.1248/yakushi1947.118.12_581.
[34] R.M.Q. Shanks, N.P. Donegan, M.L. Graber, S.E. Buckingham, M.E. Zegans, A.L. Cheung, G.A. O'Toole, Heparin Stimulates Staphylococcus aureus Biofilm Formation, Infection and Immunity. 73 (2005) 4596–4606. https://doi.org/10.1128/IAI.73.8.4596-4606.2005.
[35] EE MacKintosh, J.D. Patel, R.E. Marchant, J.M. Anderson, Effects of biomaterial surface chemistry on the adhesion and biofilm formation of Staphylococcus epidermidis in vitro, Journal of Biomedical Materials Research Part A. 78A (2006) 836–842. https://doi.org/10.1002/jbm.a.30905.
[36] S. Galliani, A. Cremieux, P. Van Der Auwera, M. Viot, Influence of strain, biomaterial, proteins, and oncostatic chemotherapy on staphylococcus epidermidis adhesion to

intravascular catheters in vitro, Journal of Laboratory and Clinical Medicine. 127 (1996) 71–80. https://doi.org/10.1016/S0022-2143(96)90168-7.
[37] S. Wu, B. Zhang, Y. Liu, X. Suo, H. Li, Influence of surface topography on bacterial adhesion: A review (Review), Biointerphases. 13 (2018) 060801. https://doi.org/10.1116/1.5054057.
[38] T. Liu, Q. Cui, Q. Wu, X. Li, K. Song, D. Ge, S. Guan, Mechanism Study of Bacteria Killed on Nanostructures, J. Phys. Chem. B. 123 (2019) 8686–8696. https://doi.org/10.1021/acs.jpcb.9b07732.